Eur Radiol (2015) 25:1294–1302
DOI 10.1007/s00330-014-3539-5

UROGENITAL

Molecular imaging of prostate cancer: translating molecular biology approaches into the clinical realm

Hebert Alberto Vargas · Jan Grimm · Olivio F. Donati · Evis Sala · Hedvig Hricak

Received: 8 August 2014 / Revised: 3 November 2014 / Accepted: 20 November 2014 / Published online: 20 February 2015
© European Society of Radiology 2015

Abstract
The epidemiology of prostate cancer has dramatically changed since the introduction of prostate-specific antigen (PSA) screening in the 1980's. Most prostate cancers today are detected at early stages of the disease and are considered 'indolent'; however, some patients' prostate cancers demonstrate a more aggressive behaviour which leads to rapid progression and death. Increasing understanding of the biology underlying the heterogeneity that characterises this disease has led to a continuously evolving role of imaging in the management of prostate cancer. Functional and metabolic imaging techniques are gaining importance as the impact on the therapeutic paradigm has shifted from structural tumour detection alone to distinguishing patients with indolent tumours that can be managed conservatively (e.g., by active surveillance) from patients with more aggressive tumours that may require definitive treatment with surgery or radiation. In this review, we discuss advanced imaging techniques that allow direct visualisation of molecular interactions relevant to prostate cancer and their potential for translation to the clinical setting in the near future. The potential use of imaging to follow molecular events during drug therapy as well as the use of imaging agents for therapeutic purposes will also be discussed.

Key Points
- *Advanced imaging techniques allow direct visualisation of molecular interactions in prostate cancer.*
- *MRI/PET, optical and Cerenkov imaging facilitate the translation of molecular biology.*
- *Multiple compounds targeting PSMA expression are currently undergoing clinical translation.*
- *Other targets (e.g., PSA, prostate-stem cell antigen, GRPR) are in development.*

Keywords Prostate cancer · Molecular imaging · MRI/PET · Optical imaging · Cerenkov imaging

Abbreviations

MRI	Magnetic resonance imaging
PET	Positron-emission tomography
SPECT	Single-photon emission computed tomography
PSMA	Prostate-specific membrane antigen
PSA	Prostate-specific antigen
PSCA	Prostate stem cell antigen
GRPR	Gastrin-releasing peptide receptor
BPH	Benign prostatic hyperplasia

Introduction

Prostate cancer is the most common cancer and the second most common cause of cancer-related death amongst men in the Americas, Europe and Australia. The role of imaging in prostate cancer is continuously evolving in parallel with increasing understanding of the underlying biological heterogeneity which characterises the disease. Functional and metabolic imaging techniques are gaining importance as the emphasis in management has shifted from structural tumour detection to accurate risk-stratification at the time of diagnosis

H. A. Vargas (✉) · J. Grimm · O. F. Donati · E. Sala · H. Hricak
Department of Radiology, Memorial Sloan Kettering Cancer Center, 1275 York Av. Room C-278, New York, NY 10065, USA
e-mail: vargasah@mskcc.org

J. Grimm
Program in Molecular Pharmacology and Chemistry, Memorial Sloan Kettering Cancer Center, 1275 York Avenue, New York, USA

O. F. Donati
Institute of Diagnostic and Interventional Radiology, University Hospital Zurich, Zurich, Switzerland

and post-treatment follow-up. Several imaging modalities are considered the key vehicles for translating molecular biology approaches into the clinical realm in prostate cancer. Technological advances in magnetic resonance imaging (MRI), positron-emission tomography (PET), optical imaging and Cerenkov imaging offer the possibility to directly visualise molecular interactions, something not achievable with standard imaging techniques [1]. These advances include the use of activatable imaging agents, which comprise the most complex of all imaging probes [2]. Through interaction with their target, activatable probes undergo a transformation that leads to a change in the emitted signal (usually, it is switched 'on' or 'off'). Thus, in contrast to targeted agents, which provide information merely about the physical presence of the target, activatable agents (often called 'smart' sensors) deliver information on the biological activity of their target [2]. Activatable agents have been devised predominantly for optical imaging applications but also for MRI. Since radioactive decay is a physical process that cannot be modified, activatable radioactive agents have long been considered impossible. However, use of the radioactive decay signal of Cerenkov light [3] may soon open the door for radiotracer-based activatable imaging agents.

Identification of a suitable molecular target

Designing imaging probes for advanced prostate cancer imaging can be challenging and involves meeting several key requirements: (1) identifying a suitable target specifically associated with prostate cancer and finding an appropriate ligand that will bind to it with high specificity; (2) labelling this ligand with a label suitable for the preferred imaging modality, which should allow for clinical translation. To find targets and ligands, various approaches can be used, including gene expression profiling and exploration of libraries. The design of the imaging probe must also take into consideration barriers it might encounter during its journey to its target. For prostate cancer, several targets have been identified, which are discussed below.

Androgen receptor (AR) imaging

Androgen deprivation therapy has played a role in the management of patients with advanced prostate cancer for over half a century [4].

Most patients with metastatic prostate cancer respond to androgen deprivation (pharmacological or surgical); however, almost invariably this is followed by progression to 'castration-resistant' disease which occurs due to 'sensitising' or 'bypassing' of the androgen receptor (AR) pathway. The AR is a ligand-dependent transcription activator which plays a key role in cell differentiation and cell proliferation [5]. The treatment of castration-resistant prostate cancer has been revolutionised in recent years by the introduction of novel therapeutic agents targeting the AR (e.g., enzalutamide) [6].

The distribution of anatomical sites where the AR is overexpressed can be imaged using the PET agent 16β-[^{18}F]fluoro-5α-dihydrotestosterone (^{18}F-FDHT) [7–9]. The differential overexpression of AR has been shown in studies comparing ^{18}F-FDHT and ^{18}F-FDG in men with castration-resistant prostate cancer which have identified different 'phenotypes' amongst these patients, including those with lesions demonstrating preferential tracer accumulation on FDHT PET (AR-predominant), preferential accumulation on FDG PET (glycolysis predominant) and mixed (i.e., uptake on both FDHT and FDG PET) phenotypes (Fig. 1) [10, 11]. A recent study evaluated the associations between morphological CT patterns, glycolytic activity and AR expression on PET and found that the numbers of bone lesions on CT, FDG PET and

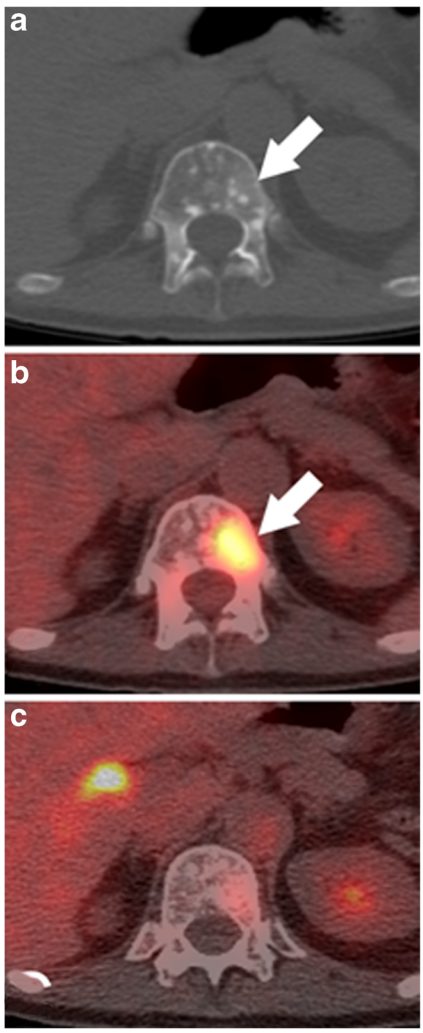


Fig. 1 Axial CT (**a**), fused FDG PET/CT (**b**) and fused FDHT PET/CT (**c**) images demonstrate the biological diversity of bone metastases in patients with castration-resistant prostate cancer. Subtle groundglass and miliary density lesion in T12 vertebral body (*arrows*), with marked glycolytic activity but minimal androgen expression, as evidenced by uptake on FDG but not on FDHT PET

FDHT PET, as well as the intensity of FDHT uptake, are significantly associated with overall survival [11].

^{18}F-FDHT could also have a potential role as a pharmacodynamic marker of drug targeting. One study reported that enzalutamide (AR receptor antagonist) induced ^{18}F-FDHT uptake changes in metastatic lesions could be considered a surrogate marker for adequate 'targeting' of prostate cancer metastases with AR overexpression [6].

Prostate-specific membrane antigen (PSMA)

Prostate-specific membrane antigen (PSMA) is probably the most prominent prostate cancer-associated antigen. It is a dimeric Type II integral membrane glycoprotein, highly expressed on prostate cancer cells [12]. Higher PSMA levels are seen in metastatic and higher-grade prostate cancer [13]. High levels of PSMA expression correlate significantly with early biochemical recurrence in surgically treated prostate cancer and also with tumour stage, Gleason grade and preoperative PSA and HER2 expression ($P<0.0001$ each) [14]. It has also been shown that the level of PSMA expression associated with benign prostatic hyperplasia (BPH) is lower than that associated with normal prostate and significantly lower than that associated with prostate cancer [15, 16]. Therefore BPH is not expected to substantially interfere with any PSMA-based methods of characterising prostatic tissue (e.g., as benign or malignant).

Conventionally, PSMA is detected using labelled monoclonal antibodies or small molecules [17, 18], which indicate the expression of PSMA protein. The most prominent of the monoclonal antibodies are 7E11 (ProstaScint®) and the more recently developed J591. In 1996, the US Food and Drug Administration approved the use of ProstaScint (indium-111 [^{111}In]-labelled capromab pendetide or 7E11, Cytogen Corporation, Princeton NJ, USA), for single-photon emission computed tomography (SPECT) imaging of soft-tissue (but not bone) sites of metastatic prostate cancer for pre-surgical staging or evaluation of prostate-specific antigen (PSA) relapse after radical prostatectomy. 7E11 is a murine mAb specific for an epitope on the intracellular domain of PSMA. In several studies, ProstaScint imaging displayed sensitivity of 60 %, specificity of 70 %, positive predictive value of 60 % and negative predictive value of 70 % for prostate cancer soft-tissue lesions [19–21]. However, the intracellular binding site of ^{111}In-7E11 is only accessible upon membrane disruption in dying or dead cells [22]. Therefore, probably because the number of available targets in the absence of membrane disruption is limited, SPECT with ^{111}In-7E11 has low sensitivity for viable tumour sites (62 % for lymph node metastases, 50 % for prostate bed recurrence). Furthermore, ^{111}In-capromab pendetide does not bind to viable prostate cancer sites in bone (the most common site of metastatic disease), and in contrast to PET, SPECT remains only semi-quantitative in the clinical setting.

For PET, a variety of appropriate radioisotopes with different properties are available and already in clinical use. The novel PET nuclide Zirconium-89 (^{89}Zr), with its unique physical decay properties and energy ($t_{1/2}$=78.43 h, β^+=22.3 %, $E_{\beta+,max}$= 901 keV, E_γ=909 keV), is ideally suited for targeted imaging probes, especially antibodies. The greater half-life provides copious activity at the required circulation times for optimal targeting to disease sites [23, 24]. The longer half-life even enables imaging at later time points, including 120 hours post injection, an imaging window difficult to achieve with the shorter-lived PET nuclides ^{18}F and ^{64}Cu [23, 25]. Recently, a new imaging approach was described for 7E11, utilising the perceived disadvantage that the recognised epitope only becomes accessible upon membrane disruption [24]. ^{89}Zr was conjugated to 7E11 to provide a radiotracer for measuring the response of prostate cancer to treatment by using biodistribution studies and immunoPET imaging. It was shown that the effects of chemotherapy, chemical castration or radiotherapy could be monitored by observing 7E11 uptake, which increased with progressing cell membrane disruption resulting from treatment-induced cell death (Fig. 2). The uptake of ^{89}Zr-7E11 correlated strongly with markers of cell death and apoptosis (Fig. 3). The results confirmed that ^{89}Zr-7E11 immunoPET could potentially be used for successful non-invasive evaluation of treatment response regardless of the type of therapy applied [24].

In contrast to 7E11, the humanised J591 monoclonal antibody targets the extracellular epitope of PSMA [26], which is available on live and dead cells alike. J591 is therefore not significantly influenced by changes in membrane permeability. It has been radiolabelled with ^{89}Zr for immunoPET imaging where it has demonstrated high tumour-to-background tissue ratios [23] (Fig. 4). Overall, the novel radiotracers ^{89}Zr-7E11 and -J591 represent promising candidates for translation to the clinic for noninvasively diagnosing prostate cancer and assessing its response to treatment. A clinical trial using J591 is currently underway (NCT01543659) as are several trials using J591 as a therapeutic agent. The radiolabelled J591 has also been used to perform targeted Cerenkov imaging in mouse models [3]. Compared to standard optical imaging approaches, Cerenkov imaging approaches using approved radiotracers offer the possibility of relatively rapid clinical translation [27]. Cerenkov radiation is produced when charged particles travel faster than the speed of light through a dielectric medium [27]. Cerenkov imaging exploits the light emission from commonly used diagnostic (e.g., all PET isotopes) and many therapeutic radionuclides [27]. This modality detects a lower amount of light compared to other optical imaging techniques such as fluorescence and bioluminescence; however, it benefits from high signal-to-noise ratios resulting from lack of incident light sources [27].

Hormone therapy is often used in the management of prostate cancer. Wright and colleagues [28] have observed that hormone deprivation leads to an increase of PSMA expression in vitro while hormone replenishment suppresses

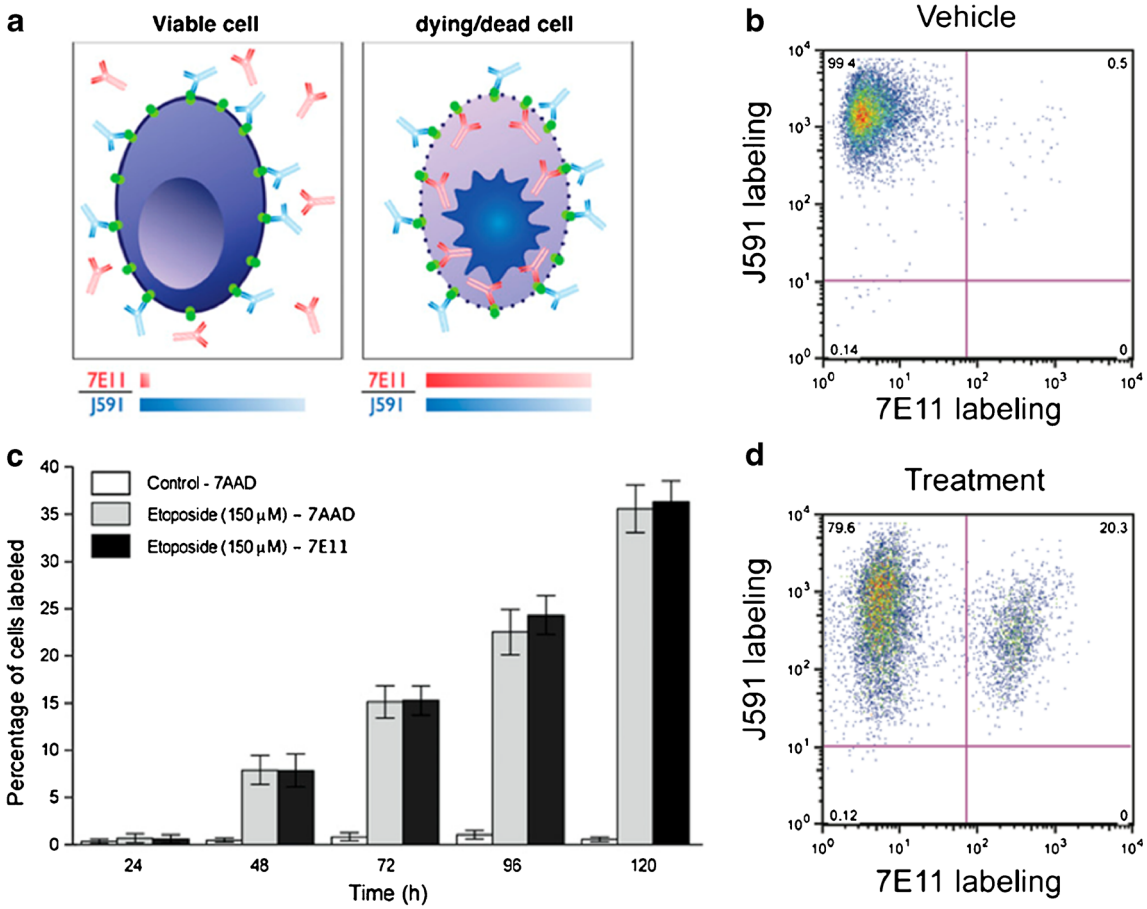


Fig. 2 PSMA+ cell responses to different treatments in vitro. **a** The monoclonal antibody 7E11 binds to an intracellular epitope of PSMA, labelling apoptotic or already dead cells, whose leaky cell membrane permits access of the antibody to the intracellular domain. **b** The monoclonal antibody J591, recognises the extracellular domain of PSMA and thus binds to all PSMA-positive cells, regardless of their viability. **c** Higher percentage of 7AAD and 7E11 stained cells is observed over time with flow cytometry after treatment compared to control ($P<0.05$). **d** Corresponding staining is observed for both 7E11 and 7AAD staining, a marker of late apoptosis (and thus cell death) after treatment with etoposide (PC3/PSMA+ cells). With permission from Ruggiero A et al. (2012) J Nucl Med 52(8):1608-15

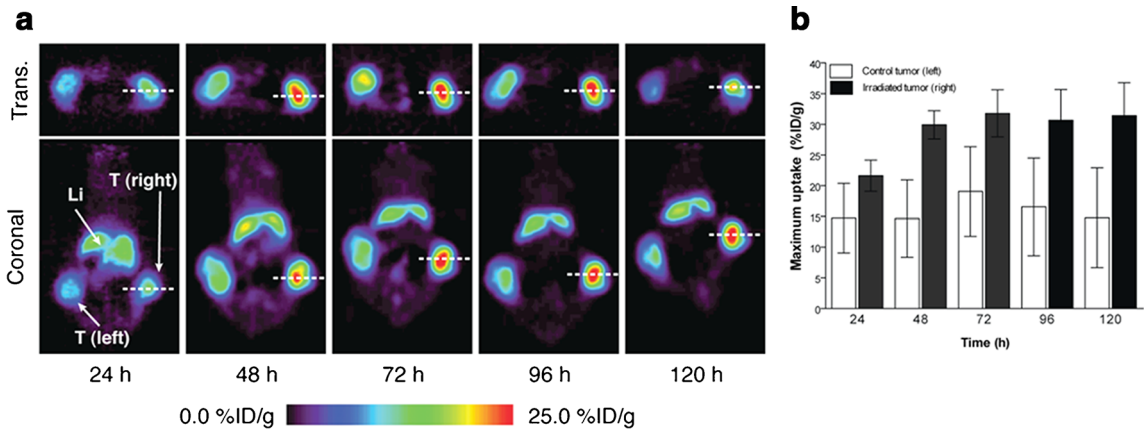


Fig. 3 In vivo imaging of therapy response with 89Zr-7E11 ImmunoPET in xenograft-bearing mice. **a** Representative transverse and coronal 89Zr-7E11 immunoPET images at different time points in a LNCaP xenograft-bearing mouse treated with selective radiation to the right side. Increased uptake of 89Zr-7E11 was observed in the selectively irradiated tumour (*right*) compared to the control (*left*). The dashed line represents the position of the perpendicularly oriented image. *T* tumour, *Li* liver. **b** 89Zr-7E11 uptake values (obtained from the PET data as maximum %ID/g) were significantly higher in irradiated than in control tumours at 24 h ($P=0.0376$), 48 h ($P=0.0009$), 72 h ($P=0.0086$), 96 h ($P=0.01$) and 120 h ($P=0.0075$). With permission from Ruggiero A et al. (2012) J Nucl Med 52(8):1608-15

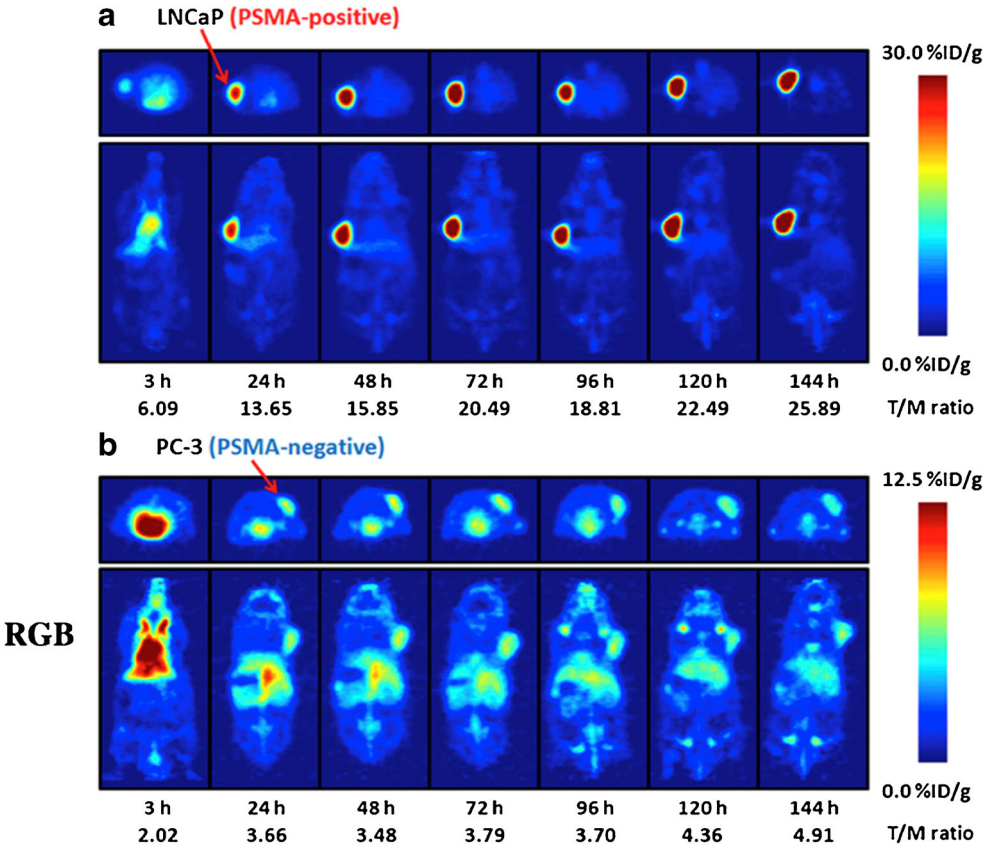


Fig. 4 Temporal immunoPET images of 89Zr-DFO-J591 (10.9–11.3 MBq [295–305 mCi], 60–62 mg of mAb, in 200 mL of sterile saline) recorded in LNCaP tumor–bearing (PSMA-positive, left shoulder) **a** and PC-3 tumour–bearing (PSMA-negative, right shoulder) **b** mice between 3 and 144 h after injection. Transverse and coronal planar images intersect centre of tumours, and mean tumour-to-muscle ratios derived from volume-of-interest analysis of immunoPET images are given. Upper thresholds of immunoPET have been adjusted for visual clarity, as indicated by *scale bars*. With permission from Holland J et al. (2012) J Nucl Med 51(8):1293-1300

PSMA expression. Recently, it was demonstrated that therapy with the new anti-androgen enzalutamide increased PSMA expression. This change in response to treatment was subsequently quantitatively measured with PET utilising radiolabelled J591 (^{64}Cu-J591) in prostate cancer xenograft models [29]. Similar findings have also been reported for PSA.

In addition to antibodies, several small molecules have been described as ligands to PSMA. Low-molecular-weight imaging agents have several inherent advantages over bigger ligands such as antibodies, including faster tumour uptake and increased clearance from non-target sites. Many low-molecular-weight inhibitors of PSMA have been reported [30–32]. A prominent example – now translated to the clinic – is N-[N-[(S)-1,3-dicarboxypropyl]carbamoyl]-4-(18)F-fluorobenzyl-L-cysteine (^{18}F-DCFBC), a small molecule inhibitor of PSMA's carboxypeptidase function [32]. As an inhibitor this small molecule binds specifically and irreversibly to PSMA's active side. Since tumour uptake and blood clearance are more rapid for small molecules than for antibodies, the pharmacodynamics of ^{18}F-DCFBC are more favourable, with higher tumour-to-background ratios; however, a moderate degree of remaining blood pool activity has been noted, possibly due to binding to serum proteins. Abnormal uptake may be noted at sites (e.g., lymph nodes) that would not be deemed metastatic based on size criteria on standard cross-sectional imaging (Fig. 5). Similar agents have been labelled with ^{123}I for SPECT imaging [33]. These compounds also demonstrate rapid distribution, blood clearance rates and tumour uptake, providing very good tumour-to-background contrast (Fig. 6). The same inhibitor has also been used for a targeted, nanoparticle-based theranostic approach [34], combining imaging and drug delivery in one entity [35]. For targeting to PSMA, this particle carried the small molecule PSMA inhibitor; for therapy, it carried the enzyme bacterial cytosine deaminase (bCD) to convert the nontoxic pro-drug 5-fluorocytosine (5-FC) to cytotoxic 5-fluorouracil (5-FU) and a vector for siRNA to downregulate choline kinase, which is overexpressed in prostate cancer. The particle was labelled for imaging with the near-infrared fluorochrome Cy5.5 for optical imaging and ^{111}In-DOTA for SPECT imaging.

Multiple optical imaging agents targeting PSMA have been developed, some utilising the J591 antibody with various light emitters, including radiotracers for Cerenkov emission [3, 36]. A few small-molecule-based fluorescent agents have been developed as well, based on either phosphoramidate or urea-based peptidomimetics [17, 37]. While these agents currently remain in the pre-clinical realm (Fig. 7), considerable efforts are underway to move them forward into clinical applications. A number of methods exist to perform whole-body tomography with fluorescent agents on animals [38], but at present there are no methods for applying this concept to whole body human scanning. Therefore, surface-based optical imaging

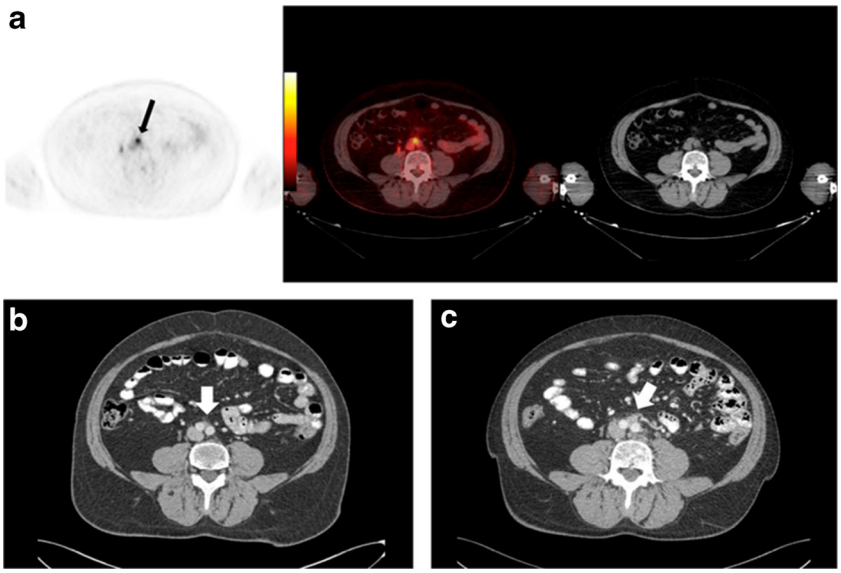


Fig. 5 Clinical PSMA imaging with fluorinated small molecule. **a** and **b** Focal 18 F-DCFBC PET uptake at aortic bifurcation (*arrow*, A) with correlative small LN seen on concurrent contrast-enhanced CT (*arrow*, B), not considered to be nodal metastasis by CT but positive by PET. **c** Retrospective review of prior contrast-enhanced CT scan obtained 1 y previously demonstrates LN in this region (*arrow*). With permission from Cho SY et al. (2012) J Nucl Med 53(12):1883-91

(mostly intraoperative and endoscopic) is being pursued [39]. Enhanced intraoperative detection of cancerous lesions has been achieved with fluorescence-guided imaging and resection, using fluorescent dyes that target tumours [39–41]. Because of superior tissue penetration and decreased autofluorescence, dyes with emission in the near-infrared (NIR) window of the spectrum (650−900 nm) are preferred.

Another promising ligand to detect PSMA is an aptamer. Aptamers are relatively short strands of oligonucleic molecules that bind to a specific target [42]. Aptamers are widely known as a substitute for antibodies, because these molecules overcome some weaknesses of antibodies. They offer high stability, facile production, low immunogenicity, rapid clearance and the possibility of binding to targets that are low in immunogenicity. An aptamer targeting PSMA (A10) has been developed [43] and has been coupled to a co-polymeric drug-delivering nanoparticle; a single intratumoral administration of the construct was significantly more efficacious in tumour reduction than were non-targeted particles and controls in animal experiments [44]. Similar constructs have been made with the toxin gelonin, resulting in 600-fold higher potency on PSMA-positive cells than that achieved with negative controls [45]. Polymeric nanoparticles containing cyanine dyes as fluorochromes have been devised for fluorescence imaging [46]. Iron oxide nanoparticles coated with the aptamer and intercalated doxorubicin have been used for MR

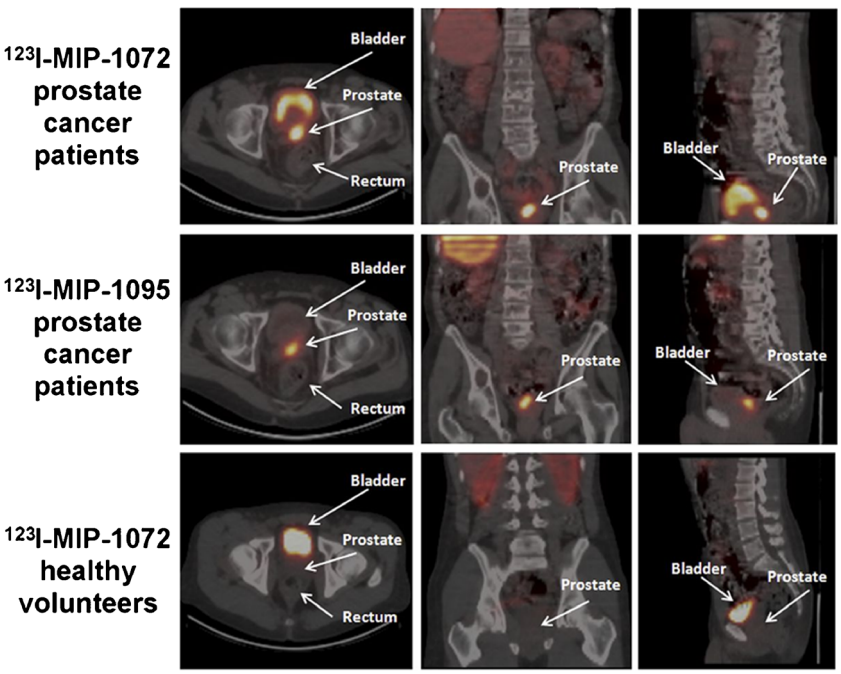


Fig. 6 Clinical PSMA imaging with iodinated small molecule. Patients with radiographically confirmed metastatic prostate cancer to whom 370 MBq (10 mCi) of 123I-MIP 1072 and 123I-MIP- 1095 were administered, and for comparative purposes, healthy volunteers to whom 370 MBq of 123I-MIP 1072 were administered. Depicted are representative transaxial (*left*), coronal (*middle*) and sagittal (*right*) slices from reconstructed SPECT/CT at 4 h after injection, demonstrating excellent depiction of the prostate tumour. With permission from Barrett JA et al. (2013) J Nucl Med 54(3):380-7

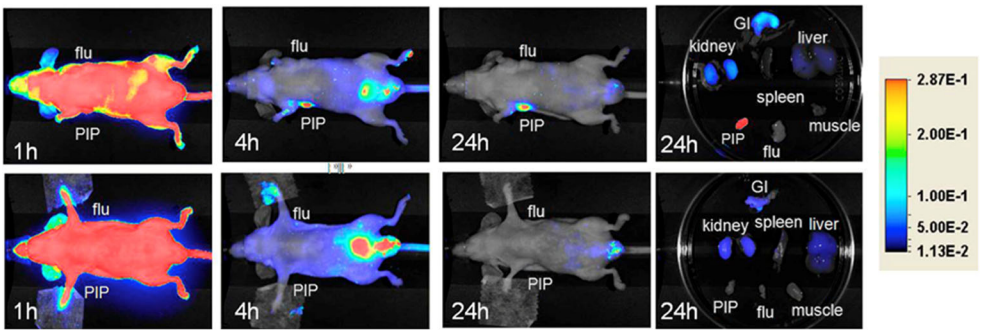


Fig. 7 Optical imaging. *Top row*: Images after administration of 1 nmol Cy7-3 at (*left* to *right*) 1, 4 and 24 h post injection, as well as images of the excised organs at 24 h post injection. *Bottom row*: Image after administration of 1 nmol Cy7-3+1 mmol DCIBzL, a high-affinity ligand for PSMA (blocker) at same time points as above. Note lack of uptake in the mice treated with DCIBzL, indicating binding specificity. With permission from Chen Y et al. (2012) Bioconjug Chem 23(12):2377-85

imaging and targeted drug delivery [47]. Recently, A10 has been radiolabelled with ^{64}Cu for possible PET imaging of PSMA-positive tumours [48].

Prostate-specific antigen (PSA)

Standard prostate cancer screening is partially based on the detection of abnormally increased serum PSA levels; however, prostate cancers are found in up to 15 % of patients with normal serum, including aggressive tumours with Gleason scores of ≥7 [49]. PSA screening therefore cannot reliably differentiate between indolent and aggressive disease [50]. Although PSA expression is tightly coupled to androgen receptor signalling and approximately 80 % to 90 % of prostate cancers are dependent on androgens, the ability to detect PSA in serum requires not only its expression within the cells but also its secretion and leakage into the circulation [51]. Only a very small amount of PSA is secreted into perivascular space and then ultimately into the serum [52]. Importantly, PSA is initially produced as an active protease ('free' PSA), and after its release into the perivascular space, it is quickly converted to its inactive forms ('complexed' PSA) [53]. A monoclonal antibody (5A10) recognising an epitope near the catalytic cleft of PSA has been developed. This antibody only binds to free PSA, which remains associated with the tumour. ^{89}Zr-labeled 5A10 has exhibited excellent tumour uptake in multiple preclinical models of prostate cancer [51]. Importantly, the androgen dependence of the PSA could be visualised with PET. In one study, therapy with increasing amounts of the anti-androgen enzalutamide demonstrated a dose-dependent depression of tumour-associated ^{89}Zr-5A10 in primary tumours as well as bone lesions, while testosterone supplementation resulted in increased binding [51]. This study provided more evidence that therapy-dependent molecular changes of AR-targeted prostate-specific genes – the expression levels of PSA [51] as well as PSMA [29] – can be quantified non-invasively with radiolabelled antibodies and PET. Since such tracers can be translated relatively quickly for clinical use, initial clinical trials are imminent.

Other targets

Several other targets on prostate cancer cells as well as on neovasculature of prostate cancers have been described. *Prostate stem cell antigen* (PSCA) is a cell surface glycoprotein, which is overexpressed in the majority of prostate cancers and prostate bone metastases. Antibodies against this antigen have been raised [54] for PET imaging, although the uptake in the tumour, at less than 5 %, was relatively low. The antigen has also been targeted with an antibody-nanoparticle construct for combined MR imaging and immunotherapy [55] or drug release [56]. Another promising target is *bombesin.* The gastrin-releasing peptide receptor (GRPR) provides a promising target for staging and monitoring prostate cancer, since it is overexpressed only in prostate cancer and not in normal prostatic tissue. Bombesin is a 14-amino-acid peptide with a high binding affinity and specificity to the GRPR [57]. Radiopharmaceuticals containing bombesin or its analogues, labelled with ^{99}mTechnetium, have been developed to target GRPR-expressing tumours for nuclear imaging, mainly with SPECT. Limited clinical studies have shown promise in detecting primary prostate cancer, nodal and bone metastases [58, 59]. Other labelling methods to obtain agents suitable for PET imaging are currently underway [60]. Fluorescently labelled versions have been evaluated in animal models [61] and could find their way into intraoperative imaging eventually.

Conclusion

Multiple molecular imaging agents for prostate cancer are currently being evaluated – most of them in preclinical settings but a few in clinical trials. In the future, quantitative radiotracers may be used not only to characterise prostate cancer and to stage disease, but also to follow molecular events during drug therapy to gauge therapeutic effectiveness

much earlier. Once approved, optical imaging agents could literally lead the surgeon to the cancer and to potential areas of invasion or metastatic lymph nodes. The result may be improved surgical resection and, hopefully, better outcomes. In addition, many of the imaging agents described have been explored for therapeutic approaches as well, either as theranostic nano-agents or for simply delivering a cytotoxic agent to the tumour. The future of molecularly driven prostate cancer diagnosis and therapy appears promising.

Acknowledgments The scientific guarantor of this publication is Hedvig Hricak. The authors of this manuscript declare no relationships with any companies whose products or services may be related to the subject matter of the article. The authors state that this work has not received any funding. No complex statistical methods were necessary for this paper. Institutional Review Board approval was not required because this was a review article.

References

1. Elias DR, Thorek DLJ, Chen AK, Czupryna J, Tsourkas A (2008) In vivo imaging of cancer biomarkers using activatable molecular probes. Cancer Biomarkers 4:287–305
2. Thorek DL, Grimm J (2012) Enzymatically activatable diagnostic probes. Curr Pharm Biotechnol 13:523–536
3. Ruggiero A, Holland JP, Lewis JS, Grimm J (2010) Cerenkov luminescence imaging of medical isotopes. J Nucl Med 51:1123–1130
4. Huggins C, Hodges CV (2002) Studies on prostatic cancer: I. The effect of castration, of estrogen and of androgen injection on serum phosphatases in metastatic carcinoma of the prostate. 1941. J Urol 168:9–12
5. Azzouni F, Mohler J (2012) Biology of castration-recurrent prostate cancer. Urol Clin N Am 39:435–452
6. Scher HI, Beer TM, Higano CS et al (2010) Antitumour activity of MDV3100 in castration-resistant prostate cancer: a phase 1-2 study. Lancet 375:1437–1446
7. Larson SM, Morris M, Gunther I et al (2004) Tumor localization of 16beta-18 F-fluoro-5alpha-dihydrotestosterone versus 18 F-FDG in patients with progressive, metastatic prostate cancer. J Nucl Med 45: 366–373
8. Beattie BJ, Smith-Jones PM, Jhanwar YS et al (2010) Pharmacokinetic assessment of the uptake of 16beta-18 F-fluoro-5alpha-dihydrotestosterone (FDHT) in prostate tumors as measured by PET. J Nucl Med 51:183–192
9. Zanzonico PB, Finn R, Pentlow KS et al (2004) PET-based radiation dosimetry in man of 18 F-fluorodihydrotestosterone, a new radiotracer for imaging prostate cancer. J Nucl Med 45:1966–1971
10. Fox JJ, Autran-Blanc E, Morris MJ et al (2011) Practical approach for comparative analysis of multilesion molecular imaging using a semiautomated program for PET/CT. J Nucl Med 52:1727–1732
11. Vargas HA, Wassberg C, Fox JJ et al (2014) Bone metastases in castration-resistant prostate cancer: associations between morphologic CT patterns, glycolytic activity, and androgen receptor expression on PET and overall survival. Radiology 271:220–229
12. Su SL, Huang IP, Fair WR, Powell CT, Heston WDW (1995) Alternatively spliced variants of prostate-specific membrane antigen Rna - ratio of expression as a potential measurement of progression. Cancer Res 55:1441–1443
13. Mannweiler S, Amersdorfer P, Trajanoski S, Terrett JA, King D, Mehes G (2009) Heterogeneity of prostate-specific membrane antigen (PSMA) expression in prostate carcinoma with distant metastasis. Pathol Oncol Res 15:167–172
14. Minner S, Wittmer C, Graefen M et al (2011) High level PSMA expression is associated with early PSA recurrence in surgically treated prostate cancer. Prostate 71:281–288
15. Chikkaveeraiah BV, Bhirde A, Malhotra R, Patel V, Gutkind JS, Rusling JF (2009) Single-wall carbon nanotube forest arrays for immunoelectrochemical measurement of four protein biomarkers for prostate cancer. Anal Chem 81:9129–9134
16. Lapidus RG, Tiffany CW, Isaacs JT, Slusher BS (2000) Prostate-specific membrane antigen (PSMA) enzyme activity is elevated in prostate cancer cells. Prostate 45:350–354
17. Chen Y, Dhara S, Banerjee SR et al (2009) A low molecular weight PSMA-based fluorescent imaging agent for cancer. Biochem Biophys Res Commun 390:624–629
18. Hillier SM, Maresca KP, Femia FJ et al (2009) Preclinical evaluation of novel glutamate-urea-lysine analogues that target prostate-specific membrane antigen as molecular imaging pharmaceuticals for prostate cancer. Cancer Res 69:6932–6940
19. Haseman MK, Reed NL, Rosenthal SA (1996) Monoclonal antibody imaging of occult prostate cancer in patients with elevated prostate-specific antigen. Positron emission tomography and biopsy correlation. Clin Nucl Med 21:704–713
20. Babaian RJ, Sayer J, Podoloff DA, Steelhammer LC, Bhadkamkar VA, Gulfo JV (1994) Radioimmunoscintigraphy of pelvic lymph nodes with 111indium-labeled monoclonal antibody CYT-356. J Urol 152:1952–1955
21. Polascik TJ, Manyak MJ, Haseman MK et al (1999) Comparison of clinical staging algorithms and 111indium-capromab pendetide immunoscintigraphy in the prediction of lymph node involvement in high risk prostate carcinoma patients. Cancer 85:1586–1592
22. Elgamal AA, Holmes EH, Su SL et al (2000) Prostate-specific membrane antigen (PSMA): current benefits and future value. Semin Surg Oncol 18:10–16
23. Holland JP, Divilov V, Bander NH, Smith-Jones PM, Larson SM, Lewis JS (2010) 89Zr-DFO-J591 for immunoPET of prostate-specific membrane antigen expression in vivo. J Nucl Med 51: 1293–1300
24. Ruggiero A, Holland JP, Hudolin T et al (2011) Targeting the internal epitope of prostate-specific membrane antigen with 89Zr-7E11 immuno-PET. J Nucl Med 52:1608–1615
25. Holland JP, Caldas-Lopes E, Divilov V et al (2010) Measuring the pharmacodynamic effects of a novel Hsp90 inhibitor on HER2/neu expression in mice using Zr-DFO-trastuzumab. PLoS One 5:e8859
26. Liu H, Moy P, Kim S et al (1997) Monoclonal antibodies to the extracellular domain of prostate-specific membrane antigen also react with tumor vascular endothelium. Cancer Res 57:3629–3634
27. Thorek D, Robertson R, Bacchus WA et al (2012) Cerenkov imaging - a new modality for molecular imaging. Am J Nucl Med Mol Imaging 2:163–173
28. Wright GL Jr, Grob BM, Haley C et al (1996) Upregulation of prostate-specific membrane antigen after androgen-deprivation therapy. Urology 48:326–334
29. Evans MJ, Smith-Jones PM, Wongvipat J et al (2011) Noninvasive measurement of androgen receptor signaling with a positron-emitting radiopharmaceutical that targets prostate-specific membrane antigen. Proc Natl Acad Sci U S A 108:9578–9582
30. Barinka C, Rovenska M, Mlcochova P et al (2007) Structural insight into the pharmacophore pocket of human glutamate carboxypeptidase II. J Med Chem 50:3267–3273
31. Mease RC, Dusich CL, Foss CA et al (2008) N-[N-[(S)-1,3-Dicarboxypropyl]carbamoyl]-4-[18 F]fluorobenzyl-L-cysteine, [18 F]DCFBC: a new imaging probe for prostate cancer. Clin Cancer Res 14:3036–3043
32. Cho SY, Gage KL, Mease RC et al (2012) Biodistribution, tumor detection, and radiation dosimetry of 18 F-DCFBC, a low-molecular-

weight inhibitor of prostate-specific membrane antigen, in patients with metastatic prostate cancer. J Nucl Med 53:1883–1891
33. Barrett JA, Coleman RE, Goldsmith SJ et al (2013) First-in-man evaluation of 2 high-affinity PSMA-avid small molecules for imaging prostate cancer. J Nucl Med 54:380–387
34. Chen Z, Penet MF, Nimmagadda S et al (2012) PSMA-targeted theranostic nanoplex for prostate cancer therapy. ACS Nano 6: 7752–7762
35. Grimm J, Scheinberg DA (2011) Will nanotechnology influence targeted cancer therapy? Semin Radiat Oncol 21:80–87
36. Nakajima T, Mitsunaga M, Bander NH, Heston WD, Choyke PL, Kobayashi H (2011) Targeted, activatable, in vivo fluorescence imaging of prostate-specific membrane antigen (PSMA) positive tumors using the quenched humanized J591 antibody-indocyanine green (ICG) conjugate. Bioconjug Chem 22:1700–1705
37. Liu T, Wu LY, Hopkins MR, Choi JK, Berkman CE (2010) A targeted low molecular weight near-infrared fluorescent probe for prostate cancer. Bioorg Med Chem Lett 20:7124–7126
38. Grimm J, Kirsch DG, Windsor SD et al (2005) Use of gene expression profiling to direct in vivo molecular imaging of lung cancer. Proc Natl Acad Sci U S A 102:14404–14409
39. van Dam GM, Themelis G, Crane LM et al (2011) Intraoperative tumor-specific fluorescence imaging in ovarian cancer by folate receptor-alpha targeting: first in-human results. Nat Med 17:1315–1319
40. Schaafsma BE, Mieog JS, Hutteman M et al (2011) The clinical use of indocyanine green as a near-infrared fluorescent contrast agent for image-guided oncologic surgery. J Surg Oncol 104:323–332
41. Schaafsma BE, van der Vorst JR, Gaarenstroom KN et al (2012) Randomized comparison of near-infrared fluorescence lymphatic tracers for sentinel lymph node mapping of cervical cancer. Gynecol Oncol 127:126–130
42. Song KM, Lee S, Ban C (2012) Aptamers and their biological applications. Sensors (Basel) 12:612–631
43. Lupold SE, Hicke BJ, Lin Y, Coffey DS (2002) Identification and characterization of nuclease-stabilized RNA molecules that bind human prostate cancer cells via the prostate-specific membrane antigen. Cancer Res 62:4029–4033
44. Farokhzad OC, Cheng J, Teply BA et al (2006) Targeted nanoparticle-aptamer bioconjugates for cancer chemotherapy in vivo. Proc Natl Acad Sci U S A 103:6315–6320
45. Chu TC, Marks JW 3rd, Lavery LA et al (2006) Aptamer:toxin conjugates that specifically target prostate tumor cells. Cancer Res 66:5989–5992
46. Tong R, Coyle VJ, Tang L, Barger AM, Fan TM, Cheng J (2010) Polylactide nanoparticles containing stably incorporated cyanine dyes for in vitro and in vivo imaging applications. Microsc Res Tech 73:901–909
47. Yu MK, Kim D, Lee IH, So JS, Jeong YY, Jon S (2011) Image-guided prostate cancer therapy using aptamer-functionalized thermally cross-linked superparamagnetic iron oxide nanoparticles. Small 7:2241–2249
48. Rockey WM, Huang L, Kloepping KC, Baumhover NJ, Giangrande PH, Schultz MK (2011) Synthesis and radiolabeling of chelator-RNA aptamer bioconjugates with copper-64 for targeted molecular imaging. Bioorg Med Chem 19:4080–4090
49. Thompson IM, Pauler DK, Goodman PJ et al (2004) Prevalence of prostate cancer among men with a prostate-specific antigen level < or =4.0 ng per milliliter. N Engl J Med 350:2239–2246
50. Lilja H, Ulmert D, Vickers AJ (2008) Prostate-specific antigen and prostate cancer: prediction, detection and monitoring. Nat Rev Cancer 8:268–278
51. Ulmert D, Evans MJ, Holland JP et al (2012) Imaging androgen receptor signaling with a radiotracer targeting free prostate-specific antigen. Cancer Discov 2:320–327
52. Stege RH, Tribukait B, Carlstrom KAM, Grande M, Pousette AHL (1999) Tissue PSA from fine-needle biopsies of prostatic carcinoma as related to serum PSA, clinical stage, cytological grade, and DNA ploidy. Prostate 38:183–188
53. Lilja H (1985) A kallikrein-like serine protease in prostatic fluid cleaves the predominant seminal vesicle protein. J Clin Invest 76: 1899–1903
54. Lepin EJ, Leyton JV, Zhou Y et al (2010) An affinity matured minibody for PET imaging of prostate stem cell antigen (PSCA)-expressing tumors. Eur J Nucl Med Mol Imaging 37:1529–1538
55. Ren J, Wang F, Wei G et al (2012) MRl of prostate cancer antigen expression for diagnosis and immunotherapy. PLoS One 7:e38350
56. Gao X, Luo Y, Wang Y et al (2012) Prostate stem cell antigen-targeted nanoparticles with dual functional properties: in vivo imaging and cancer chemotherapy. Int J Nanomedicine 7:4037–4051
57. Smith CJ (2003) Radiochemical investigations of gastrin-releasing peptide receptor-specific [(99 m)Tc(X)(CO)3-Dpr-Ser-Ser-Ser-Gln-Trp-Ala-Val-Gly-His-Leu-Met-(NH2)] in PC-3, tumor-bearing, rodent models: syntheses, radiolabeling, and in vitro/in vivo studies where Dpr=2,3-diaminopropionic acid and X=H2O or P(CH2OH)3. Cancer Res (Baltimore) 63:4082–4088
58. De Vincentis G, Remediani S, Varvarigou AD et al (2004) Role of 99mTc-bombesin scan in diagnosis and staging of prostate cancer. Cancer Biother Radiopharm 19:81–84
59. Scopinaro F, De Vincentis G, Varvarigou AD et al (2003) 99mTc-bombesin detects prostate cancer and invasion of pelvic lymph nodes. Eur J Nucl Med Mol Imaging 30:1378–1382
60. Honer M, Mu L, Stellfeld T et al (2011) 18 F-labeled bombesin analog for specific and effective targeting of prostate tumors expressing gastrin-releasing peptide receptors. J Nucl Med 52:270–278
61. Cai QY, Yu P, Besch-Williford C et al (2012) Near-infrared fluorescence imaging of gastrin releasing peptide receptor targeting in prostate cancer lymph node metastases. Prostate. doi:10.1002/pros.22630:n-a-n/a